IEEE Access
Multidisciplinary | Rapid Review | Open Access Journal

Received January 23, 2019, accepted February 3, 2019, date of publication February 13, 2019, date of current version March 1, 2019.

Digital Object Identifier 10.1109/ACCESS.2019.2899214

Investigation of Spray Angle Measurement Techniques

IRENE RUIZ-RODRIGUEZ, RADBOUD POS, THANOS MEGARITIS, AND LIONEL CHRISTOPHER GANIPPA

Mechanical Aerospace and Civil Engineering Department, Brunel University London, London UB8 3PH, U.K.

Corresponding author: Irene Ruiz-Rodriguez (irene.ruizrodriguez@brunel.ac.uk)

This work was supported by the Engineering and Physical Sciences Research Council, U.K.

ABSTRACT The in-cylinder fluid-dynamic processes of fuel injection and air entrainment influence the structure and shape of evolving fuel sprays, which can subsequently alter the ignition, combustion, and pollutant formation processes in diesel engines. Different spray angle detection methods have been used in the literature to investigate the global and local spray characteristics. In this paper, the five most widely used diesel spray angle detection methods were identified and used to evaluate the characteristic features of each detection method: methods with a detection range based on the spray penetration length, methods with a fixed detection range in the near- and far-field spray regions, triangular-based methods, and methods based on averaging local data points. The sprays were acquired from our spray chamber and processed with different thresholding techniques to explore the differences between the spray angle detection methods. All five methods generated a similar global trend of spray angle variation for temporally evolving sprays over the complete injection period. However, the actual spray angle values detected by each method were not always comparable. The differences in spray angle values between the different detection methods were larger during the early start of injection, and these differences systematically decreased as the spray approached a steady state. The methods that detected the angle in the far field demonstrated lower spatio-temporal variability when compared with the methods that detected the angle in the near field. An assessment of the comparability between angle detection methods was made, and the outcome provides guidance for the selection of the spray angle detection method.

INDEX TERMS Diesel engines, fossil fuels, image processing, spray angle measurement.

I. INTRODUCTION

Diesel engines are fuel efficient with low CO_2 emissions, and they are of paramount importance for the energy industry and for the sector of heavy-duty vehicles, as there is no reliable alternative for road and waterborne transportation. In conventional diesel engines, fuel is injected at high pressures into the cylinder where it mixes with air to form an ignitable mixture that subsequently undergoes diffusion dominated combustion [1]. Despite its advantages, soot and NOx emitted from diesel engines are of concern. Significant breakthrough has happened with exhaust after-treatment research, which reduces soot and NOx to very low levels [2]. However, the load on exhaust after-treatment systems can be reduced by improving the in-cylinder processes of combustion and emission formation, which are strongly influenced by fuel injection, air entrainment and spray development processes.

The injected high pressure diesel sprays go through different temporal stages that can be broadly classified into four regimes. The first regime is the start of injection (SOI), where a 'mushroom head' forms as fuel leaves the nozzle because of the residual fuel in the nozzle sac [3]. The transient regime follows, which covers from the SOI to the time instant at which the needle inside the nozzle reaches a fully open position. In this transient, quasi-steady regime, the spray starts to exchange momentum with the surrounding gas [4]. The third regime is the stable one, where most of the fuel is injected and the spray tends to remain in a steady-state mode until the needle starts to close. The fourth regime is the end of injection (EOI), where the needle starts to close and fuel injection terminates [5]. The spray angle changes throughout these

The associate editor coordinating the review of this manuscript and approving it for publication was Aysegül Ucar.

different regimes owing to changes in the nozzle sac flow, momentum, and the associated fuel-air interaction changes.

A generic description of the spray morphology is shown conceptually in Fig. 1. For a developed spray, two main regions can be identified: the main (conical) region of the spray and the leading edge (elliptical) part of the spray [6]–[9]. The main region occupies approximately 70% of the spray penetration, and has a sub-region called the momentum (or characteristic) length of ≈200 times the nozzle diameter [8]. The characteristic length is a sub-region where the volume of the gas entrained into the spray can be considered to be negligible [7], [8].

These high pressure diesel sprays are generally evaluated through various optical techniques such as: shadowgraphy, Schlieren, scattering, laser induced fluorescence, ballistic imaging, and X-ray imaging techniques [1], [10]–[18]. The acquired images are normally subject to analysis using any appropriate image processing software to extract global spray parameters such as spray penetration length (S), drop size distribution, and spray angle (θ) [6].

The spray angle is an important parameter that helps understand the spray's global characteristics. Direct imaging of sprays and the evaluation of the spray angle and volume through image processing can provide useful information about the global air entrainment in sprays [5], [19], [20]. Thus, the spray angle is an indicator of how much gas is entrained into a spray, which controls the extent of fuel-air mixing, vaporization, combustion and ultimately NOx and particulate matter (PM) emissions [21], [22].

If image processing techniques are used to characterize mixing in a spray, this characterization becomes somewhat dependent on the value obtained for the spray angle. Many methods exist in literature to measure diesel spray angles, and some of the most widely adopted ones are:

- #1 Fitting tangent lines to the spray edges to detect the angle as a function of the spray penetration [23]–[26]
- #2 Fitting tangent lines to the spray edges to detect the angle as a function of the nozzle geometry [27]–[31]
- #3 Calculating the angle from the spray's equivalent triangular area [5], [32], [33]
- #4 Fitting the tangent lines to the spray with the coincident point free to move [34]
- #5 Measuring the angle locally along the spray and then averaging these values for every time instant [35]

The spray angle values obtained with these methods are often used to validate spray models used in CFD. The methods can be either near or far-field, and a distinction must be made between both as they are measuring different regions of the spray.

High-speed imaging is widely used to evaluate spray morphology, as it allows for a global spatio-temporal characterization of events such as radial expansions in the spray, end of injection expulsions and wall impingement. The flexibility that it offers in terms of low maintenance cost and easy adaptability to realistic practical combustion systems makes it a popular technique for spray characterization [36]–[38].

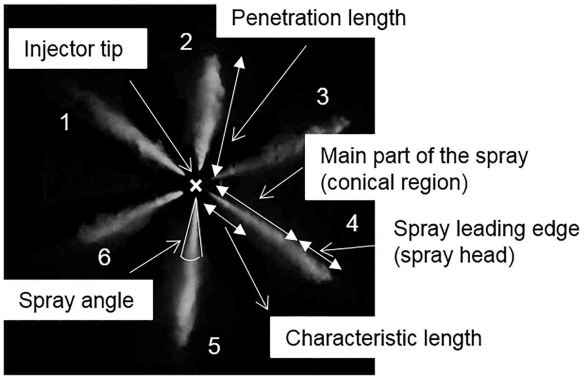

FIGURE 1. Definition of generic spray parameters-pointers and markers are not to scale.

It is therefore important to refine the image analysis processes that are used to extract spray data. One such parameter of interest is the spray angle, which, as aforementioned, can be detected in several different ways. Understanding how the different spray angle detection methods affect the output is critical when it comes to interpreting the data presented in different works.

The strategy used to detect diesel spray angles is different for each method. Very limited information is available in the literature to elucidate the differences between the detection methods and to assess their sensitivity in detecting spray angles for the early start of injection, for the quasi-steady state, and for the steady state regime. In this paper, an in-depth study of the strategies adopted in some of the most widely used methods (#1 to #5) and their ability to detect spray angles for the early start, quasi-steady state, and steady state spray regimes will be discussed. The injection-to-injection variability of each method was assessed in terms of the standard deviation, and a study was made on how the methods adapted to radial expansions that appear in transiently evolving sprays. Additionally, we explored how the relative differences between angle detection methods changed with different spray boundary thresholding techniques.

The paper is organized as follows: the experimental methods are presented in §2; a description of the spray angle detection methods is provided in §3; the results and discussions are presented in §4; and the conclusions are presented in §5.

II. EXPERIMENTS AND SPRAY ANALYSIS

The spray data required to evaluate the methods (#1 to #5) were obtained by injecting diesel fuel into a constant volume chamber (CVC). The CVC was filled with nitrogen to a pressure of 30 bar ± 2 bar and heated to 116°C ± 2°C to avoid window fouling due to fuel condensation. Diesel was injected at 800 bar using a 6-hole common rail injector. The spray development was acquired at 45000fps (frames per second) at a resolution of 512 pixels x 512 pixels using a high-speed CMOS camera. The set-up is shown in Fig. 2 and full details of the set-up can be found in [39]. The illumination and

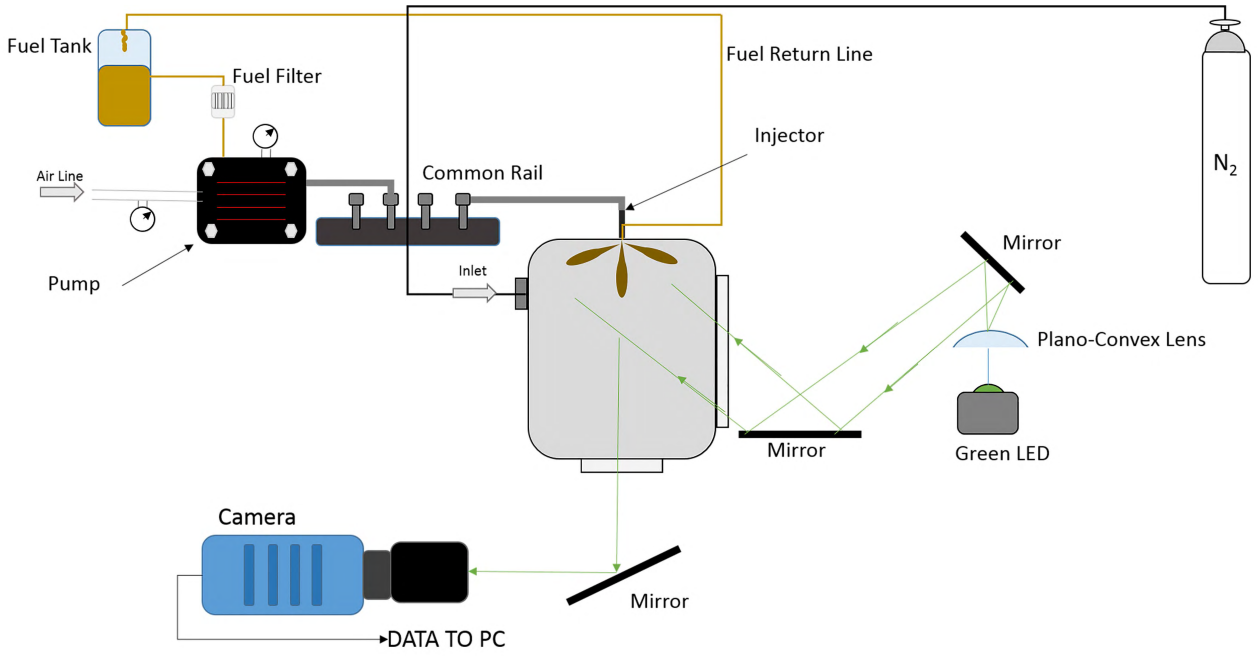

FIGURE 2. Schematic of the experimental set-up.

the camera set-up were optimized to obtain the maximum spatio-temporal resolution of spray 4, hence only spray 4, as shown in Fig. 1, was considered for the evaluation of the spray angle.

In order to obtain statistically significant data, 12 injections were performed. Thus, for each spray angle measurement method, the spray angle values were obtained for 12 injection events. The number of injections considered in this study are adequate for spray analysis as highlighted in [14], [23], [24], [29], and [33]. The variability of the methods was studied by using the angle's standard deviation (SD), where a smaller SD indicates less sensitivity to injection-to-injection variations.

In addition to these measurements, spray data under the same operating conditions from three more injectors of the same type were used (with permission of [37]). These injectors were obtained from vehicles that had done mileages of 30, 000, 60, 000, and 90, 000 on UK roads and were prone to deposit and wear, which can affect the spatio-temporal variations of the spray structure. Details of these injectors and their spray characteristics can be seen in [37]. These additional spray data were used to investigate the capability of each spray angle detection method (#1 to #5) to adapt to radial expansions in the spray.

The acquired spray images were post-processed with an in-house developed C++ code implemented in Matlab. Along the spray edges, the intensity of the scattered light changes due to the changing drop size distribution and spurious reflections from the background. This makes locating the spray boundaries challenging, and is a critical step that affects the measurement of the spray angle value. The spray edge detection relies heavily on the threshold used for binarization [10], [40]–[42], and different edge-detection techniques can incur variations of up to 24% on the measured spray angles when the same measurement method is used [41]. Locating the spray boundary is a research subject of its own [43]–[45], and various approaches have been used in the literature [10], [40], [41]. Since the main emphasis of this work was to study the outcome of different spray angle detection methods, it was desirable to keep the edge detection scheme consistent for each injection.

The images acquired were corrected for dark current and background noise, and then segmented into 6 individual sprays. This was followed by grayscaling of the sprays and then binarization using an average OTSU method. In this work, the above binarization scheme was consistently adopted to extract the spray contour used to determine the spray angle. However, the influence of the thresholding technique on the relative differences between each spray angle measurement method was also explored, and the results are presented in §4A. To demonstrate the thresholding effects, in addition to the OTSU method, the spray data was also processed using two additional thresholding techniques: maximum entropy thresholding and fixed thresholding at 10% of the maximum brightness. Details of these thresholding methods can be found in [46] and [47] and in [48] and [49]. As done for the OTSU thresholding procedure, the same extracted spray was used to fit the spray angle detection methods. For visualization purposes, the boundaries obtained using the OTSU, maximum entropy and maximum brightness thresholding techniques have been overlaid on the single shot spray explored in §4A, and is shown in Fig. 3.

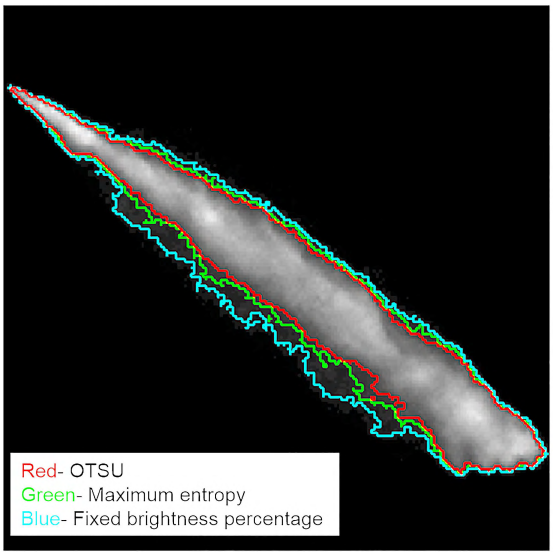

FIGURE 3. Schematic of the different thresholding techniques used in this study. The OTSU technique was the one carried through in the whole study. Brightness and contrast adjusted for visualization purposes.

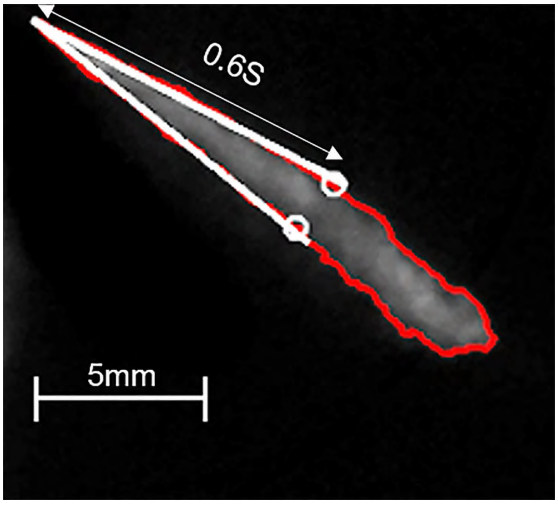

FIGURE 4. Method #1. Tangent lines used to detect the spray angle, extending from the spray origin up to 60% of the spray tip penetration length. Brightness adjusted by 61%. Angle value: 12.8° (OTSU), 16.8° (Maximum entropy), 20.8° (Brightness percentage).

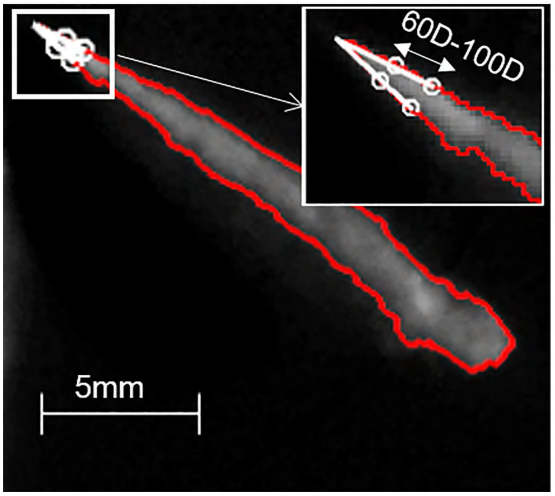

FIGURE 5. Method #2. Tangent lines fixed at 60D-100D from the nozzle orifice. Brightness adjusted by 61%. Angle value: 19.4° (OTSU), 24.2° (Maximum entropy), 27.6° (Brightness percentage).

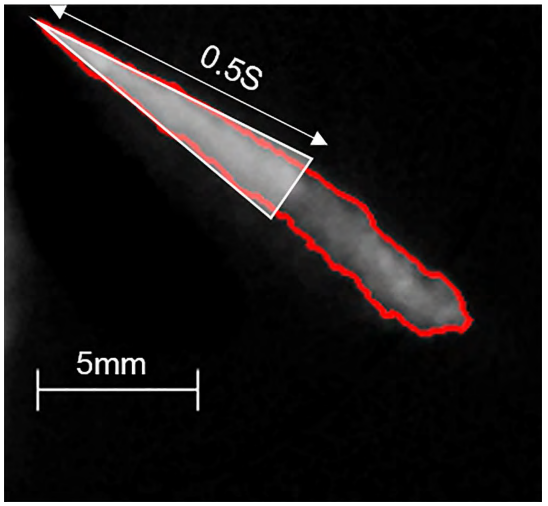

FIGURE 6. Method #3. Representation of the equivalent spray area of an isosceles triangle with a height of 50% of the penetration length used to obtain the angle. Brightness adjusted by 61%. Angle value: 16.3° (OTSU), 21.3° (Maximum entropy), 25.4° (Brightness percentage).

III. SPRAY ANGLE DETECTION METHODS

The principles of the methods used in this work to evaluate the spray angle (#1 to #5) are discussed in this section. The features of each spray angle detection method are conceptually represented in Fig. 4 to Fig. 8, for a spray acquired at 154μs after the start of injection (aSOI).

A. LINE FITTING AS A FUNCTION OF THE SPRAY TIP PENETRATION LENGTH (METHOD #1)

This method is based on measuring the angle between two lines fitted to the spray edges, where a least-square technique is used to determine the best fit of these lines. The lines extend from the spray's origin to a downstream distance relative to the spray penetration length. The lines' origin is normally fixed at the tip of the nozzle [5], [23], [25], [26], [38], [50], although some studies exist that fix the origin at a virtual position, located just upstream from the nozzle tip [42].

The penetration length up to which the lines are fitted to the spray edges varies in different publications, with values of 50% or 60% being the most common [5], [23], [25], [26], [38], [50]–[53]. These percentages are chosen to avoid the spray leading edge affecting the angle values [25], and it has been noted in [40] that the spray angle values obtained at 45%, 50% or 60% of the spray penetration do not vary significantly. The application of this method to a single spray is shown in Fig. 4, which resulted in a spray angle value of 12.8° when 60% of the spray penetration was considered

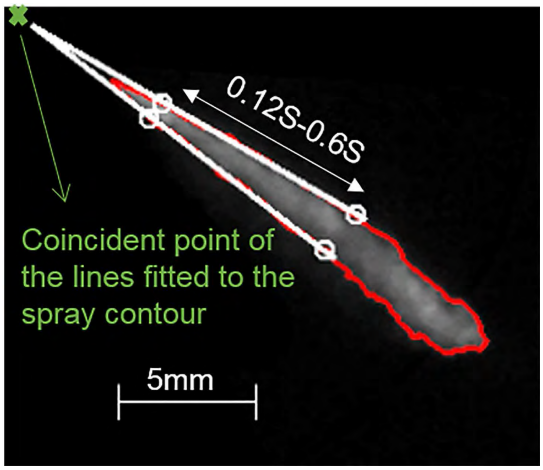

FIGURE 7. Method #4. Lines fitted between two points without fixing them at the spray's origin. Lines fitted between 12% and 60%. Brightness adjusted by 61%. Angle value: 9.5° (OTSU), 12.6° (Maximum entropy), 15.2° (Brightness percentage).

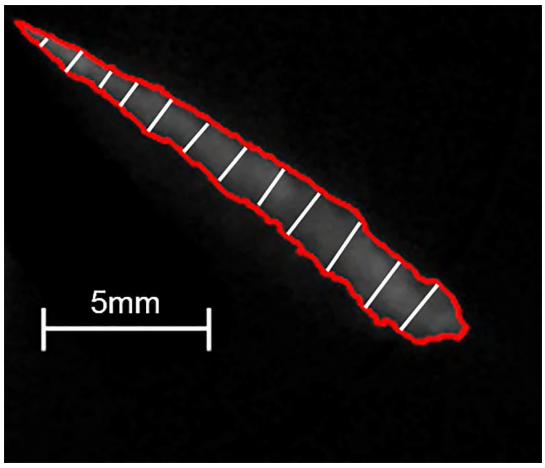

FIGURE 8. Method #5. Representation of some locations at which the angles were detected and averaged to obtain a single averaged value. Brightness adjusted by 61%. Angle value: 12.1° (OTSU), 17.5° (Maximum entropy), 20.8° (Brightness percentage).

for line fitting. When using the maximum entropy thresholding method for boundary detection, the angle value was 16.8°, and when using the brightness percentage thresholding it was 20.8°.

B. LINE FITTING AS AN EXPLICIT FUNCTION OF THE INJECTOR GEOMETRY (METHOD #2)

This method is similar to that discussed in §3A, but the penetration distance up to which the lines are fitted to the spray edges is explicitly defined in terms of multiples of the injector orifice diameter (D). Normally, two locations in terms of the orifice diameter are chosen, and the lines are fitted starting from a fixed origin and passing through the two locations following a best linear fit (Fig. 5).

In the previous method (method #1), the angle varies with respect to the development of the spray as the measurement lines follow the spray growth. In this method (method #2), since the measurement location is fixed at a defined distance from the nozzle, variation of the angle is only provided at a fixed range of the spray. As a result, this method is useful for understanding localized events in the spray but will not fully capture the global spray development.

In literature, various multiples of the injector diameter ranging from 10D to 100D as well as fixed downstream distances are used as locations to fit the lines to the spray edges [27]–[31]. Fixing the measurement distance independent of time can result in loss of information of the initial spray development until the spray reaches the selected points. The selection of the measurement locations will normally depend on the spray region of interest, so care must be taken when comparing angles evaluated at different locations. Sometimes a combination of two fixed measurement ranges have been used in literature to characterize both 'near' and 'far' field spray angles to provide a comprehensive picture of the spray [27], [54], [55]. The application of this measurement method with fixed measurement locations at 60D and 100D resulted in a spray angle value of 19.4°, as shown in Fig. 5. When using the maximum entropy thresholding method for boundary detection, the angle value was 24.2°, and when using the brightness percentage thresholding it was 27.6°.

C. TRIANGLE-BASED METHODS (METHOD #3)

The triangle method is based on constructing an isosceles triangle with an apex at the nozzle tip and a height of 50% of the penetration length [11], as shown in Fig. 6. The spray angle is defined as the apex angle of a triangle with the same projected area to that of the spray. A variation of this method based on the measured spray volume was proposed in [56], where a cone with a base diameter of half an ellipse at 0.5S was used [56]. The application of this method resulted in a spray angle value of 16.3°, as shown in Fig. 6. When using the maximum entropy thresholding method for boundary detection, the angle value was 21.3°, and when using the brightness percentage thresholding it was 25.4°.

D. FLEXIBLE TWO-POINT METHOD (METHOD #4)

This method measures the angle between lines fitted from a virtual origin through two sets of points along the spray edge. Points can be selected based on a fixed distance in terms of nozzle diameters [27]–[31], in terms of an arbitrary distance from the nozzle [8], [51], or in terms of a percentage of the penetration length [23], [25], [26], [34], [42], [50]–[53], [57]. These points are normally selected to cover the spray region where the angle is of interest.

Unlike methods #1 and #2, for the flexible two-point method the intersection location of the lines fitted to the spray edges is not fixed, and it may or may not coincide with the nozzle tip. By not fixing the origin at the nozzle tip, the lines fitted to the spray edge have the flexibility to move and the angle becomes sensitive to the region selected for line fitting rather than a global spray representation. Selecting the region

for line fitting closer to the spray's origin could provide a larger angle value as the virtual origin will tend to move downstream of the spray, whereas selecting it closer to the spray head can result in lower values, as the virtual origin tends to move upstream.

For a generic representative value of the spray, the set of points used for line fitting were placed at 12% and 60% of the penetration length. The application of this flexible two point method resulted in a spray angle value of 9.5°, as shown in Fig. 7. When using the maximum entropy thresholding method for boundary detection, the angle value was 12.6°, and when using the brightness percentage thresholding it was 15.2°.

E. LOCAL AND AVERAGED SPRAY ANGLE (METHOD #5)

This method detects the spray angle at selected vector points from the spray's origin to a defined downstream distance of the spray [35]. As with the other methods, it provides one angle value for every point in time, however, this value corresponds to the average of many angles measured at different spatial locations throughout the spray at that specific point in time. The selection of downstream points used for line fitting can be done using the aforementioned methods (method #1 or #2). The angle detection is normally done using the isosceles triangle method (method #3) or by fitting lines to the spray edge (method #1 and #2). In this work, the last downstream location for fitting of the lines was at the end of the spray within the field of view (FoV), with the spray angle at any time instant being the average of 50 equally distributed measurement locations. To obtain a single representative value of the spray angle, the average of all the local spray angles has to be obtained, which results in a computationally demanding method [35]. Applying this method to the spray used in this section resulted in a spray angle value of 12.1°, as shown conceptually in Fig. 8. When using the maximum entropy thresholding method for boundary detection, the angle value was 17.5°, and when using the brightness percentage thresholding it was 20.8°. A brief study on the computational cost of each method was performed, and this method took $\approx$8 times more to process than the other methods, which had similar processing times. When processing large amounts of data this can become an important consideration in assessing which method to use.

Several other spray angle detection methods can be found in the literature, and some of these methods are briefly discussed below but are not included in this work. The trapezium method is an adapted version of the triangle method, where instead of calculating the angle from the projected triangle, a trapezium area projection is used [38]. Another method that can be found in literature is based on obtaining the spray angle as a sum of left and right half angles from the spray's middle axis [36], [58]. The angle is measured between a line tangent to one of the spray edges and a line running through the centroid's axis [36]. This is done for both sides of the spray and both values are then summed to obtain the full angle, resembling the method used in the Gasoline-Direct Injection (G-DI) standards [59]. This approach has been used when the spray's central axis was not coincident with the nozzle's hole, such as in extremely cavitating flows [36], [60].

IV. RESULTS AND DISCUSSION

This section is divided into 5 sub-sections: §4A, where the impact of thresholding on each of the spray angle detection methods has been presented; §4B, where a single shot in time was chosen to evaluate how the spray angle detection methods reflect the spray angle value in the quasi-steady regime; §4C, where the spray angle variations during the fuel injection period were investigated to evaluate how the methods captured the spray angle variations with time; §4D, where the method's variability was assessed in terms of the standard deviation; and §4E, where each method's capability of adapting to radially expanding sprays has been discussed.

A. EFFECT OF THRESHOLDING ON ANGLE VALUES

Even though this paper focuses on how the principles behind the implementation of each spray angle detection method affect the angle values, the effect of changing the boundary thresholding technique was also briefly explored. The spray angle detection methods described in §3 have been applied to the spray data obtained at 198μs aSOI for the three thresholding techniques discussed in §2. The thresholding analysis revealed that the quantitative value of the spray angle for each of the spray angle detection methods varied, and these findings are in line with the works of [40] and [41]. The quantitative information for the spray angle values obtained with each method and for the three thresholding techniques used in this work has been presented in Table 1.

From the results obtained, it can be seen that regardless of the spray boundary thresholding technique used, the trend of the spray angle was similar relative to each angle detection method, where generally: method #2a measured the largest values, followed by method #3, method #1, method #5, method #2b and finally method #4. When comparing the differences between the minimum and maximum spray angle values obtained from all of the five spray angle detection methods, for each of the thresholding techniques used in this work the differences were between 88% to 95%. When the near-field method (method #2a) was excluded and only far-field methods were considered, the range became 55% to 63%. This indicates that the differences between the minimum and maximum angle values measured using the different spray angle detection methods varied by less than 15% between the different thresholding techniques studied. These findings clearly portray that the selection of an appropriate spray angle detection method is important, but also that using a different thresholding technique for the detection of the spray angle can induce quantitative variations, which should not be ignored.

Subsequent results presented in §4B, §4C, §4D and §4E will be focusing on the implementation, sensitivity, and capability of each of the spray angle detection methods for a single shot, for transiently evolving sprays and for radially

TABLE 1. Description of the methods studied and the average spray angle values of 12 injection events obtained for each method with their corresponding SD at 198μs aSOI. Values obtained using the different thresholding methods are also shown.

Method number	Method details	Spray angle average at 198μs aSOI		
		OTSU threshold	Maximum entropy threshold	Brightness percentage threshold
#1	Line fitting as a function of the spray tip penetration length (at 0.6S)	12.5°± 0.7°	15.5°±1.0°	18.7°± 1.5°
#2a	Line fitting as an explicit function of the injector geometry (at 60D and 100D)	19.1°± 2.1°	22.8°± 2.3°	25.5°± 3.4°
#2b	Line fitting as an explicit function of the injector geometry (at 100D and 700D)	11.6°± 1.7°	15.6°± 0.9°	18.7°± 1.0°
#3	Triangular-based method (at 0.5S)	15.2°± 1.2°	18.9°± 1.7°	22.2°± 2.1°
#4	Two-point method with a non-fixed origin (at 0.12S and 0.6S)	9.8°± 1.7°	12.0°± 2.7°	13.6°± 3.2°
#5	Local and averaged spray angle (for 12 locations)	11.9°± 0.8°	15.3°± 1.3°	18.0°± 1.9°

expanding sprays. Henceforth, a single consistent boundary thresholding technique based on the OTSU technique was adopted.

B. SINGLE SHOT SPRAY ANGLE ANALYSIS

The spray angle detection methods studied and the corresponding values for the spray angle determined at 198μs aSOI are summarized in Table 1. This time instant was chosen because the spray was approaching the steady state condition and the differences between methods were more obvious than in the steady state regime.

It is important to note that not all methods detected the angle on the same spray region. For example, when looking at the values at 198μs aSOI, method #1 detected an average spray angle value of 12.5°, which corresponds to the main (conical region) of the spray, whereas method #2a detected an average spray angle value of 19.1°, but in the near-nozzle region for the same spray. Extending the reach of the detection region of method #2a from the near nozzle region (between 60D and 100D) to method #2b (between 100D and 700D) changed the value of the spray angle from 19.1° to 11.6°. This change in near and far nozzle angle values was caused by the linear fitting method used to detect both angles. The larger distance between the points used for the measurement in method #2b caused the linear fit of the measuring lines to subtend a smaller angle in-between when compared to that of method #2a. This shows that, when using the same line fitting method for angle detection, angles detected at different spray locations are not necessarily comparable. Differences in near and far nozzle angle values have also been observed in [27], [54], and [55].

Method #3 used a portion of the spray with a downstream reach similar to that in method #1, however, as the angle was computed from an equivalent triangular area, the value was larger. Method #4 also detected the angle in a spray region based on the spray penetration in a manner similar to that in method #1. However, it did so obviating the near nozzle region for the fit of the detection lines and allowing these lines to be coincident elsewhere than at the origin. The latter explains the lower spray angle value of method #4 when compared to that obtained using method #1, as for method #4 the coincident point of the detection lines at 198μs moved upstream of the spray resulting in a smaller angle. When studying the outcome of method #5, the spray angle value at 198μs resembled that of method #1, even though method #5 accounted for the spray head for the computation of the angle. This is because most of the points selected for angle detection were located on the conical region of the spray, and this had a larger weighting than the points on the spray head region.

For the single shot analysis of the spray angle presented in Table 1, the angle detection range along the spray for method #1 was varied to cover a similar detection range to that of methods #2a and #2b. As mentioned in §3B, for method #2 the origin was fixed and the remaining two locations were fitted using a best linear fit. When changing the detection range of method #1 to one similar to methods #2a and #2b, the angle obtained was within 5% and 1% of the values produced by methods #2a and #2b respectively. This shows that if the detection range of method #1 is similar to that of #2 the methods produce comparable spray angle values for a given time instant. However, this is only the case for a single shot in time because, when looking at the time-varying spray, method #2 detects the angle at the exact same location regardless of spray growth. On the other hand, the detection range in method #1 is dependent on the spray penetration length and thus the angle detected is relative to the spray growth. This observation also highlights that for a fixed

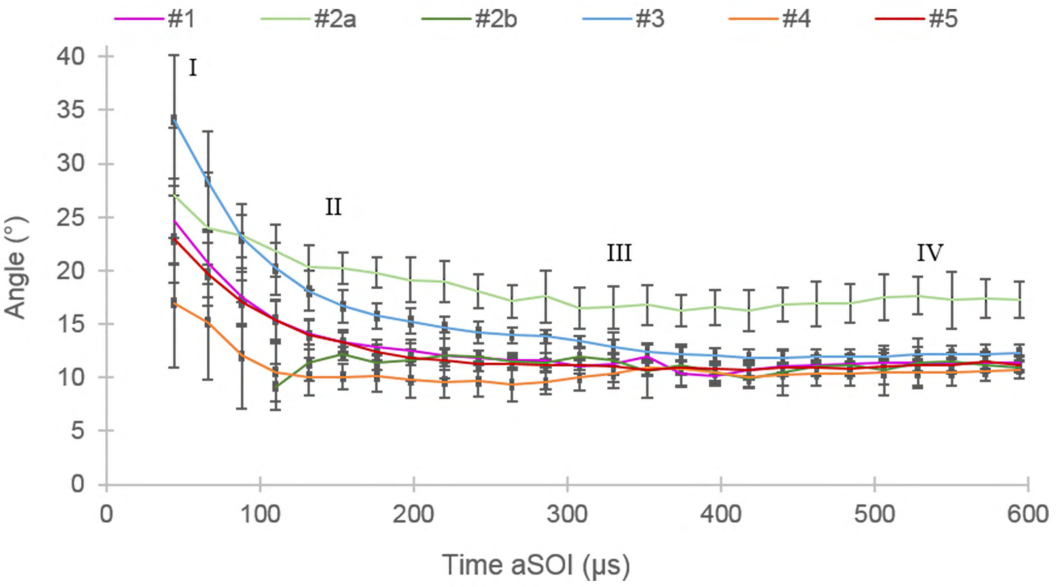

(a)

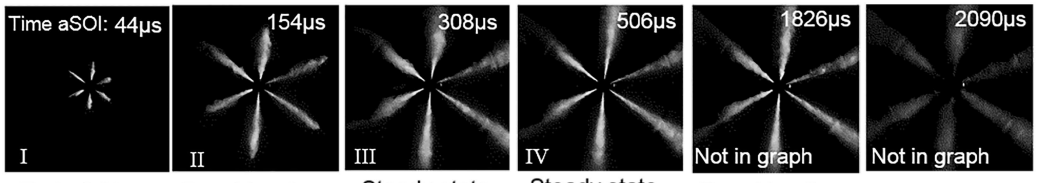

Early SOI larger angles observed | Reaching the end of the SOI, approaching steady state | Steady state reached, angle remains constant | Steady state, angle remains constant | Reaching the EOI (needle close), angle widens | After the needle has fully closed, sprays dispersing

(b)

FIGURE 9. a) Angle variation with respect to time for the methods studied. Each data point represents an ensemble average of 12 injections. b) A sequence of spray images from the needle opening to the needle closing phase, showing the general trend in angle variation (LED illuminates from right to left). The Roman numerals in the images correspond to the region indicated in a). Brightness enhanced by 70%.

origin and a comparable spray detection range, performing a 2-point (origin, location 1) or 3-point (origin, location 1 and location 2) best linear fit to the spray edge for angle detection does not a cause significant difference in the angle value.

From the analysis of a single shot in the quasi-steady state regime, it is clear that the spray angle values determined using methods #1, #2b and #5 produced a comparable value of ≈12°, while method #4 produced a slightly smaller value of ≈10°. Method #2a consistently produced a larger value of ≈19° and method #3 produced a value of ≈15°. Method #2a produced the largest value, but it measured the angle in the near-nozzle and therefore characterized a different portion of the spray than the other methods that measured at the far-field of the spray. Nonetheless, a difference of 2° to 9° exists in spray angle values between methods for the point in time selected. In practical terms this means that, if a spray angle value is used to quantify the air entrainment [5], [19], [20], different spray angle values produced by different methods could lead to over or under estimations of the true air entrainment - and this can subsequently lead to variations in emissions predictions.

C. TRANSIENT SPRAY ANGLE VARIATIONS

In the previous section, a single point in time was chosen to illustrate how different detection methods can produce different spray angle values for a given spray. Extending this single shot in time to an injection period provides information on the relative temporal variations of the spray angle when different methods are used, as shown in Fig. 9a and 9b. The optical window in the chamber enabled the visualization of the full spray up to 300μs aSOI. This limited the study of those spray angle detection methods that relied on a percentage of S for the measurement of the angle. Once the spray tip was out of the FoV, the S value could not be measured, hence Hiroyasu and Arai's spray penetration model [6] with modifications to accommodate additional geometric characteristics of the

nozzle from [61], was used to calculate S after 300μs aSOI. As a result, the analysis could be extended to the point in time where 60% of the spray penetration length had reached the end of the FoV.

This allowed the analysis to be extended up to 594μs aSOI, which corresponded to the time instant at which 60% of the calculated S reached the end of the FoV for the set injection pressure and ambient conditions. After this, the analysis was stopped, as methods using a percentage of S would no longer detect angles representative of the spray. In order to validate the model, spray penetration data obtained from the model was compared to the experimentally measured spray penetration before the spray reached the end of the FoV. The uncertainty was less than 6%, and thus its impact on the measurement of the spray angle was considered to be negligible.

The first ≈300μs aSOI accounted for the needle lifting phase, point after which the needle remained in an open position and closed at ≈1300μs aSOI. As seen in Fig. 9a, a distinctive trend of the spray angle variation was consistently observed for all the methods, which is similar to the one observed in earlier works on spray angles [5], [30], [52], [62]. During the initial needle opening transient period, the angle is relatively large and it gradually decreases during the needle lifting phase as the spray tends to reach a quasi-steady regime. Initially, as the needle is lifting, the flow of fuel through the injector orifice is restricted by this needle movement. This causes a slower fuel injection rate, which results in a larger spray angle [5]. Thereafter, when the needle reaches a fully open position, the spray eventually reaches the steady state regime. At this point, the fuel flow is no longer restricted by needle throttling, which results in a larger axial momentum and a decreased angle value when compared to the initial needle lifting phase. Finally, as the needle starts to close during the EOI, the flow rate decreases and the spray angle increases as the fuel loses momentum (the spray angle variation in this phase is not shown in Fig. 9a or 9b and is not discussed in this paper). As can be seen, changes in the spray morphology can be closely linked to the needle dynamics as well as to air entrainment [63].

Investigating the spray angle variation during the early start, quasi-steady, and early steady state regime provides an insight into how the methods compare to each other. From Fig. 9a it can be seen that method #2a measured the largest spray angle values. The large values observed for method #2a have been related to the behavior of the line-fitting approach adopted in the close proximity of the injector (between 60D and 100D). It was discussed in §4B that extending the reach of the line-fitting range (as in method #2b) causes a narrowing of the angle due to the best-fit lines fitting more tightly to the spray. This finding implies that, for the same line-fitting method and for the same angle detection method (method #2), the extent and reach of the angle detection lines can influence the output value. Therefore, a distinction must be made between near and far-field measurement methods when comparing values in the literature. It is also noted that

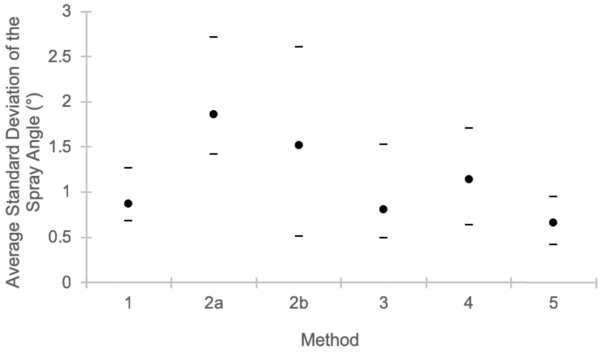

FIGURE 10. SD values obtained by averaging the SD of the 12 injection events for a period between 154μs to 594μs. The circular bold markers denote the average and the line markers the maximum and minimum SD values.

the larger spray angle values determined by method #2a may not be a true representation of the global spray but rather of the near-nozzle physics of the spray. Following method #2a, method #3 detected the second largest spray angle values. This is because when using the projected area in the calculation of the angle, parts of the spray that would not normally be accounted for when fitting lines to the spray contour were included in the angle calculation.

When assessing the methods (excluding method #2a), from Fig. 9a it can be seen that after ≈150μs, in the quasi-steady state, differences between the methods became smaller, with an average difference of 3° between the methods. This is in contrast to the 12° difference between the methods observed during the early start of injection. When looking at the steady-state regime, after ≈300μs aSOI, the differences became even smaller with a maximum average difference of 1.8°. From this, it is clear that the largest differences in spray angle values occurred before a steady state was reached, point after which the angle values were comparable between methods. Thus, in the next two paragraphs, the differences are assessed only from the early start of injection until 300μs aSOI.

Method #4 showed the lowest spray angle values for times <300μs aSOI. This is because the coincident point of the lines fitted for angle detection was not fixed at the spray's origin. This freedom caused the coincident point to move mostly upstream from the origin, resulting in this method detecting the smallest spray angle values. Closely following method #4, method #2b detected the smallest spray angle values.

Methods #1 and #5 produced similar spray angle values, albeit with method #5 producing values around 3% smaller. The similarity in values occurred because both methods had the coincident point of the detection lines fixed at the origin and because both had detection lines fitted to a similar range of the spray. Whilst for method #5 the spray angle values were the result of the average at many locations ranging from the start to the end of the spray, as the conical part occupied most of the spray it had a larger weighting on the average, which resulted in both methods having comparable values.

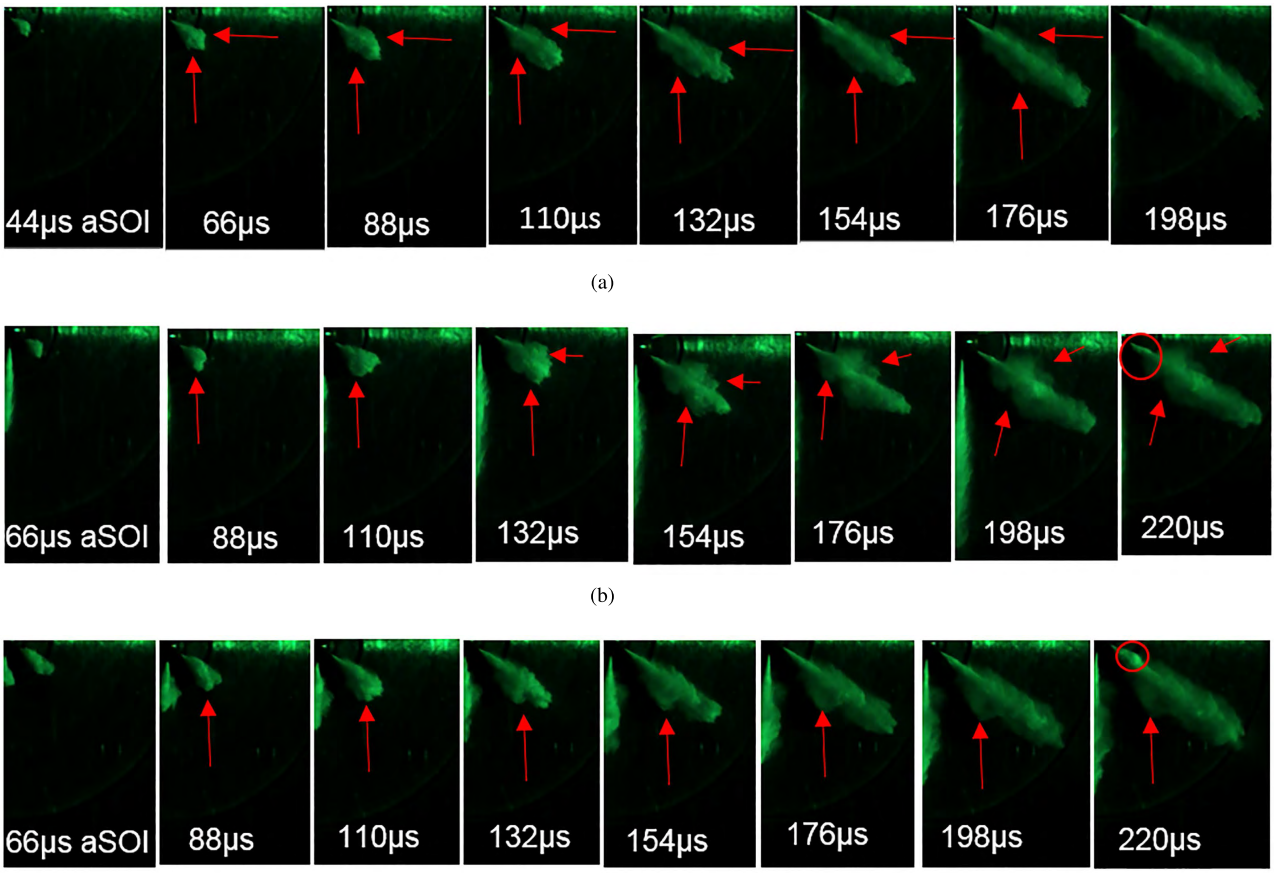

FIGURE 11. Image sequence corresponding to graphs 12 a) to c). The bulges in the spray are pointed out with an arrow. a) 30, 000 mileage injector. b) 60, 000 mileage injector. c) 90, 000 mileage injector. Each frame rate step corresponds to 22μs.

When assessing the sprays in the early steady state regime, from $\approx 300\mu$s aSOI onwards, the spray angle values produced by all methods converged to a value of approximately $11° \pm 1°$ (except method #2a which measured the angle in the near-field). This observation shows that in the steady state regime most methods produce comparable values and that values produced by different methods can be cross-compared between studies. For the chosen ambient and injection conditions studied, this value was consistent with the theory of [56] and [64], whereby using their model to calculate the spray angle in the steady state regime produces a value of $\approx 10°$.

For the three spray regimes identified in this study, the spray angle values obtained through different methods are comparable only within the steady state regime, as wide deviations exist between the methods (besides #1 and #5) during the SOI and needle opening period.

D. VARIATION BETWEEN METHODS

Injection-to-injection variations exist even under the same ambient and injection conditions. It was found that these variations were captured to a different extent by each spray angle detection method. The variations within and between methods have been presented in Fig. 10, where the circular bold markers denote the average and the line markers represent the maximum and minimum SD values for the range studied. This data was obtained by averaging the SD values shown in Fig. 9a for the quasi-steady and early steady state regime for each of the 12 injection events. So, each SD data point presented in Fig. 10 is an average of 252 data points. The maximum and minimum SD represented as line markers are the maximum and minimum values that the SD takes throughout the 12 injection events. It is therefore representative of the SD range that each method held during the period studied. Fig. 10 thus shows the level of variation between methods, where the SD captures how the methods adapt spatio-temporally to local and global spray changes caused by either injection-to-injection variations or due to fuel-air interactions. This can be used to characterize the sensitivity of each method.

It can be seen from Fig. 9a and Fig. 10 that methods #1, #3 and #5 had relatively small SD values. For method #1 the average SD was 0.9°. This low SD was a result of the method detecting the angle mostly in the stable (conical) part of the spray, which means that small changes in the placement of the boundary will not affect the spray angle value considerably. For method #3, the average SD was 0.8°. For this method, as the angle was calculated from the projected spray area,

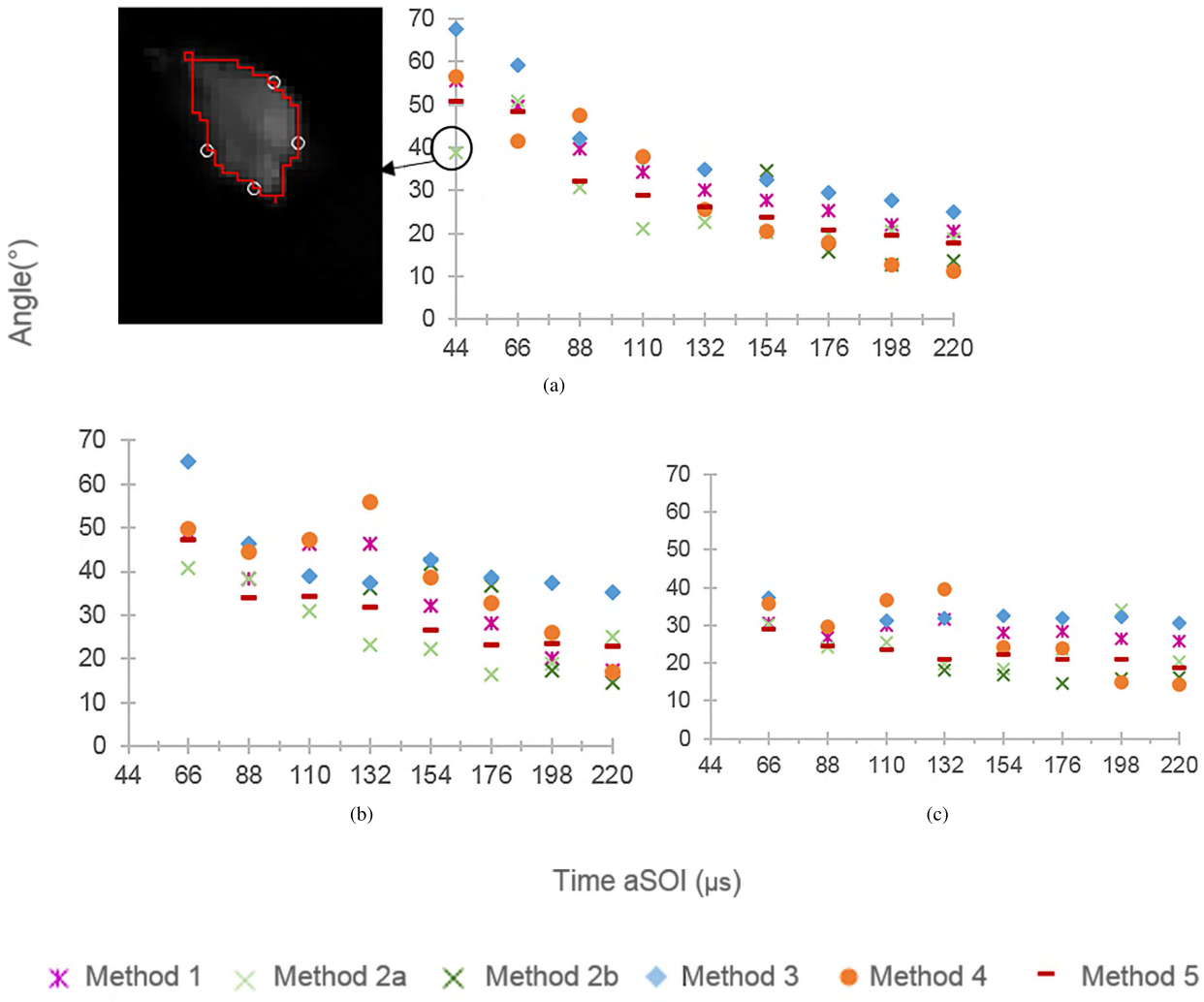

FIGURE 12. The angle evolution for the period of time when the bulges were observed, as can be seen in Figure 11 a) to c). a) 30, 000 mileage injector. b) 60, 000 mileage injector. c) 90, 000 mileage injector.

small changes in spray morphology at the boundaries were unlikely to alter the spray area, and thus the spray angle value. Method #5 also had a low variability, with an average of 0.7°. From §3E, it can be recalled that the spray angle values for this method were obtained by taking the average of the angles detected at several spray locations. This smooths out small changes in the spray boundary caused by injection-to-injection variations, which explains the low SD values shown in Fig. 10.

Method #2a had the largest SD value, with an average of 1.9°. This high SD value was a result of: firstly, fixing the detection range, which made the method more sensitive to local transients caused by injection-to-injection variations, and secondly, a result of using a small line fitting range, which caused the method to be more sensitive to variations at the boundary. After method #2a, method #2b and #4 had the largest SD values with averages of 1.5° and 1.1° respectively. For method #2b the high SD values were caused by fixing the detection region in space (not varying with spray evolution), which made this method more sensitive to variations in the spray in a similar way to method #2a. For method #4, the high variability was a result of not fixing the coincident point of the detection lines at the spray's origin, which allowed the lines fitted to the spray contour to move freely with the boundary.

Qualitatively, the SD data presented in Fig. 10 shows that the methods respond differently to local and global spatio-temporal variations.

E. METHODS' CAPABILITIES OF ADAPTING TO RADIALLY EXPANDING SPRAYS

Due to the complexities of the internal flow in the nozzle as well as the fuel-air interaction, there could be uneven spreading or local vortex bursting that can lead to radial protrusions in the spray, especially in used injectors [4], [39]. These radial distributions of mass in the sprays are referred to as bulges in [39], and this term was also adopted in this work. In this section, we studied the robustness and flexibility of the spray angle detection methods in incorporating these bulging

events while detecting the spray angle. The capability of each method to detect the spray angle for sprays that have random radial expansions will thus be discussed.

To study each of the methods' capabilities, three isolated bulging events detected from used injectors that have done 30, 000, 60, 000, and 90, 000 miles were obtained from [39]. The radial bulges were observed in the sprays at different distances from the nozzle tip, as shown in Fig. 11. For the 30, 000 set, the spray images were chosen for a time range from 44μs aSOI to 198μs aSOI (a); for the 60, 000 set, the spray images were chosen for a time range from 66μs aSOI to 198μs aSOI (b); and for the 90, 000 set, the spray images were chosen for a time range from 66μs aSOI to 220μs aSOI (c).

Generally, when bulges appeared most methods experienced an increase in spray angle value when compared to the expected baseline of a standard spray (compare Fig. 9a and Fig. 12). The results revealed that all methods showed the same behavior when bulges of comparable size appeared simultaneously on both sides of the spray, where an increase in overall spray angle value was observed. For method #2a, due to its small detection range near the nozzle, bulges went undetected in most occurrences unless they were present within its detection region. When looking closely at the first spray image, as seen in the exploded image in Fig. 12a, due to the asymmetry caused by the blob of liquid leaving the nozzle during the very early phase of injection, a spurious data point was obtained for method #2a. One of the measurement points was on a trough of the liquid blob and this caused an apparently small angle. This suggests that for detection methods based on line-fitting through points, if the point lies on a trough, the angle value might not reflect the true physics of the spray.

When bulges appeared on both sides but not simultaneously, or they appeared only on one side of the spray, methods #1 and #4 behaved similarly and detected the presence of larger bulges, as seen in Fig. 11b to 11c and 12b to 12c. When the bulge appeared for the first time, and was large relative to the spray, both methods experienced a local increase in spray angle value (88μs to 132μs). As the bulge grew along with the spray, its presence was reflected in the overall increase in spray angle values rather than as a localized increase at a point in time (see 154μs onwards). This behavior was similar to that observed for method #2b, albeit method #2b did not detect any bulges that appeared before its detection range window ($\approx$132μs). For method #2a, an increase in angle was only appreciated when the bulge was present within its detection range, as seen circled in Fig. 11b to 11c at 220μs and appreciated by an increase in angle value at 220μs in the Fig. 12b to 12c.

Method #3 reflected the appearance of a bulge by consistently detecting a larger spray angle value. Since the angle was obtained from the projected triangular area of the spray, the bulge increased the spray area radially (at the expense of the spray penetration, as seen in [39]). This produced a larger equivalent triangular area, resulting in a consistently larger spray angle value, as seen in Fig. 11b to 11c and 12b to 12b.

Method #5 smoothed out the radial variations due to the bulges, as this method computes the angle by averaging the angle values at several locations along the spray. A slight overall increase in angle value was noted when compared to the data in Fig. 9a only when the bulge was sufficiently large along the axial direction. It is postulated that for bulges that do not grow along the spray's axial direction significantly, the bulge might go undetected when using this method.

Whilst this analysis was purely qualitative, it can be stated that different methods have different capabilities of adapting to spray radial anomalies. The extent to which the bulge is detected depends on the procedure used for angle detection and on the detection range. Methods using a similar detection range detected the bulges to a similar extent, and those using the same procedure but different detection ranges detected the bulges only when they were present within the detection range.

V. CONCLUSIONS

In this work, the detection capabilities and sensitivity of five different spray angle detection methods were assessed for high pressure diesel sprays from the early start of injection until the steady state regime. The main findings can be listed as follows.

The global trend between the spray angle detection methods was similar regardless of the spray boundary thresholding technique used.

The largest difference between methods occurred at the early start of injection with a maximum of 12° (excluding near-field methods). These differences then decreased to a maximum of 3° during the quasi-steady state regime and decreased even further to less than 2° in the steady state regime.

Method #3 (the triangular method) produced the largest angle values and method #4 (flexible two-point method) produced the smallest values.

The injection-to-injection variability in terms of the SD was not captured in the same way by all methods. Methods #1, #3 and #5 (detecting the angle as a function of the spray penetration, triangle-based method and the averaging method) had the smallest injection-to-injection variability, which indicates they are more suited for generic global spray angle studies.

When bulges appeared in the spray, methods #1 and #4 detected the presence of larger bulges, whereas method #3 showed a constant increase in angle value with respect to the baseline when the bulge occurred. Method #5 smoothed out the bulges making identification of bulging complex if solely looking at the spray angle data. The behavior of methods #2a and #2b (methods with a fixed detection range) was intricate and was dependent on where and when the bulge appeared.

The findings demonstrate that the spray angle values obtained using different methods are comparable during the steady state regime but not so during the early injection period. Depending on the application as well as on the region

of interest, care must be exercised when selecting the spray angle measurement method.

REFERENCES

[1] J. E. Dec, "A conceptual model of DI diesel combustion based on laser-sheet imaging," SAE Tech. Paper 970873, Feb. 1997.
[2] K. Mollenhauer and H. Tschoeke, *Handbook Diesel Engines*. Berlin, Germany: Springer-Verlag, 2010.
[3] C. Crua, T. Shoba, M. Heikal, M. Gold, and C. Higham, "High-speed microscopic imaging of the initial stage of diesel spray formation and primary breakup," SAE Tech. Paper 2010-01-2247, Oct. 2010.
[4] R. Pos, "Spatio-temporal evolution of diesel sprays using high speed optical diagnostics," Ph.D. dissertation, CEDPS, Brunel Univ. London, London, U.K., 2016.
[5] J. Naber and D. L. Siebers, "Effects of gas density and vaporization on penetration and dispersion of diesel sprays," SAE Tech. Paper 960034, Feb. 1996.
[6] H. Hiroyasu and M. Arai, "Structures of fuel sprays in diesel engines," SAE Tech. Paper 900475, Feb. 1990.
[7] D. Tomohisa, S. Takagishi, J. Senda, and H. Fujimoto, "Organized structure and motion in diesel spray," SAE Tech. Paper 970641, Feb. 1997.
[8] T. Dan, T. Yamamoto, J. Senda, and H. Fujimoto, "Effect of nozzle configurations for characteristics of non-reacting diesel fuel spray," SAE Tech. Paper 970355, Feb. 1997.
[9] J. M. Desantes, R. Payri, F. J. Salvador, and V. Soare, "Study of the influence of geometrical and injection parameters on diesel sprays characteristics in isothermal conditions," SAE Tech. Paper 0913, Apr. 2005.
[10] R. Payri, F. J. Salvador, F. Payri, and V. Bermúdez, "The influence of cavitation on the internal flow and the spray characteristics in diesel injection nozzles," *Fuel*, vol. 83, nos. 4–5, pp. 419–431, Mar. 2004.
[11] J. M. Desantes, J. V. Pastor, R. Payri, and J. M. Pastor, "Experimental characterization of internal nozzle flow and diesel spray behavior. Part II: Evaporative conditions," *Atomization Sprays*, vol. 15, no. 5, pp. 517–544, 2005.
[12] S. Moon *et al.*, "Ultrafast X-ray phase-contrast imaging of high-speed fuel sprays from a two-hole diesel nozzle," in *Proc. 22nd Annu. Conf. Liquid Atomization Spray Syst.*, vol. 22, May 2010, pp. 1–7.
[13] G. Gong, C. Song, and L. Liu, "Spray characteristics of diesel fuel, Fishch-Tropsch diesel fuel and their blend," in *Proc. IEEE Int. Conf. Elect. Control Eng.*, Sep. 2011, pp. 4079–4082.
[14] R. J. H. Klein-Douwel, P. J. M. Frijters, L. M. T. Somers, W. A. D. Boer, and R. S. G. Baert, "Macroscopic diesel fuel spray shadowgraphy using high speed digital imaging in a high pressure cell," *Fuel*, vol. 86, nos. 12–13, pp. 1994–2007, Aug. s2007.
[15] D. Deshmukh, A. M. Mohan, T. N. C. Anand, and R. V. Ravikrishna, "Spray characterization of straight vegetable oils at high injection pressures," *Fuel*, vol. 97, pp. 879–883, Jul. 2012.
[16] E. W. Eagle, S. B. Morris, and M. S. Wooldridge, "High-speed imaging of transient diesel spray behavior during high pressure injection of a multi-hole fuel injector," *Fuel*, vol. 116, pp. 299–309, Jan. 2014.
[17] C. Wang, F. Liu, and X. Li, "Experimental research on the characteristics of dense spray of diesel engine," in *Proc. IEEE Int. Conf. Comput. Distrib. Control Intell. Environ. Monit.*, Feb. 2011, pp. 428–432.
[18] D. Wu, W. Wang, Z. Pang, S. Cao, and J. Yan, "Experimental investigation of spray characteristics of diesel-methanol-water emulsion," *Atomization Sprays*, vol. 25, no. 8, pp. 675–694, 2015.
[19] D. L. Siebers, "Scaling liquid-phase fuel penetration in diesel sprays based on mixing-limited vaporization," SAE Tech. Paper 0528, 1999.
[20] M. Arai, "Diesel spray behaviour and air entrainment," *JNNA*, vol. 2, no. 1, pp. 1–17, 2018.
[21] D.-R. Rhim and P. V. Farrell, "Effect of gas density and the number of injector holes on the air flow surrounding non-evaporating transient diesel sprays," SAE Tech. Paper 0532, 2001.
[22] M. P. B. Musculus and K. Kattke, "Entrainment waves in diesel jets," SAE Tech. Paper 1355, 2009.
[23] J. Kang, C. Bae, and K. O. Lee, "Initial development of non-evaporating diesel sprays in common-rail injection systems," *Int. J. Engine Res.*, vol. 4, no. 4, pp. 283–298, Aug. 2003.
[24] R. Payri, F. J. Salvador, J. Gimeno, and J. de La Morena, "Macroscopic behavior of diesel sprays in the near-nozzle field," *SAE Int. J. Engines*, vol. 1, no. 1, pp. 528–536, 2009.
[25] L. M. Pickett, J. Manin, C. L. Genzale, D. L. Siebers, M. P. B. Musculus, and C. A. Idicheria, "Relationship between diesel fuel spray vapor penetration/dispersion and local fuel mixture fraction," *SAE Int. J. Engines*, vol. 4, no. 1, pp. 764–799, 2011.
[26] S. H. Park, S. H. Yoon, and C. S. Lee, "Effects of multiple-injection strategies on overall spray behavior, combustion, and emissions reduction characteristics of biodiesel fuel," *Appl. Energy*, vol. 88, no. 1, pp. 88–98, Jan. 2011.
[27] P. V. Farrell, C. T. Chang, and T. F. Su, "High pressure multiple injection spray characteristics," SAE Tech. Paper 960860, 1996.
[28] J. Shao, Y. Yan, G. Greeves, and S. Smith, "Quantitative characterization of diesel sprays using digital imaging techniques," *Meas. Sci. Technol.*, vol. 14, no. 7, pp. 1110–1116, Jun. 2003.
[29] J. Shao and Y. Yan, "Digital imaging based measurement of diesel spray characteristics," *IEEE Trans. Instrum. Meas.*, vol. 57, no. 9, pp. 2067–2073, Aug. 2008.
[30] Y. Jung, J. Manin, S. Skeen, and L. M. Pickett, "Measurement of liquid and vapor penetration of diesel sprays with a variation in spreading angle," SAE Tech. Paper 0946, Apr. 2015.
[31] P. Dong, K. Nishida, T. Inaba, and Y. Ogata, "Characterization of internal flow and spray behaviors of hole-type nozzle under tiny and normal injection quantity conditions for diesel engine," *SAE Int. J. Fuels Lubricants*, vol. 9, no. 1, pp. 125–137, Apr. 2016.
[32] F. Payri, R. Payri, M. Bardi, and M. Carreres, "Engine combustion network: Influence of the gas properties on the spray penetration and spreading angle," *Exp. Therm. Fluid Sci.*, vol. 53, pp. 236–243, Feb. 2014.
[33] D. R. Emberson, B. Ihracska, S. Imran, and A. Diez, "Optical characterization of diesel and water emulsion fuel injection sprays using shadowgraphy," *Fuel*, vol. 172, pp. 253–262, May 2016.
[34] R. Payri, J. P. Viera, V. Gopalakrishnan, and P. G. Szymkowicz, "The effect of nozzle geometry over internal flow and spray formation for three different fuels," *Fuel*, vol. 183, pp. 20–33, Nov. 2016.
[35] C. Du, M. Andersson, and S. Andersson, "Effects of nozzle geometry on the characteristics of an evaporating diesel spray," *SAE Int. J. Fuels Lubricants*, vol. 9, no. 3, pp. 493–513, Nov. 2016.
[36] Z. He, Z. Shao, Q. Wang, W. Zhong, and X. Tao, "Experimental study of cavitating flow inside vertical multi-hole nozzles with different length-diameter ratios using diesel and biodiesel," *Exp. Therm. Fluid Sci.*, vol. 60, pp. 252–262, Jan. 2015.
[37] R. Pos, R. Cracknell, and L. Ganippa, "Transient characteristics of diesel sprays from a deposit rich injector," *Fuel*, vol. 153, pp. 183–191, Aug. 2015.
[38] R. Payri, J. Gimeno, G. Bracho, and D. Vaquerizo, "Study of liquid and vapor phase behavior on Diesel sprays for heavy duty engine nozzles," *Appl. Therm. Eng.*, vol. 107, pp. 365–378, Aug. 2016.
[39] R. Pos, R. Wardle, R. Cracknell, and L. Ganippa, "Spatio-temporal evolution of diesel sprays at the early start of injection," *Appl. Energy*, vol. 205, pp. 391–398, Nov. 2017.
[40] J. V. Pastor, J. Arrégle, and J. M. García, and L. D. Zapata, "Segmentation of diesel spray images with log-likelihood ratio test algorithm for non-Gaussian distributions," *Appl. Opt.*, vol. 46, no. 6, pp. 888–899, 2007.
[41] V. Macian, R. Payri, A. Garcia, and M. Bardi, "Experimental evaluation of the best approach for diesel spray images segmentation," *Experim. Techn.*, vol. 36, no. 6, pp. 26–34, Nov./Dec. 2011.
[42] E. Delacourt, B. Desmet, and B. Besson, "Characterisation of very high pressure diesel sprays using digital imaging techniques," *Fuel*, vol. 84, nos. 7–8, pp. 859–867, May 2005.
[43] J. Canny, "A variational approach to edge detection," in *Proc. AAAI*, Aug. 1983, pp. 54–58.
[44] C. Lopez-Molina, B. de Baets, and H. Bustince, "Quantitative error measures for edge detection," *Pattern Recognit.*, vol. 46, no. 4, pp. 1125–1139, Apr. 2013.
[45] B. Peng, L. Zhang, X. Mou, and M. H. Yang, "Evaluation of segmentation quality via adaptive composition of reference segmentations," *IEEE Trans. Pattern Anal. Mach. Intell.*, vol. 39, no. 10, pp. 1929–1941, Oct. 2017.
[46] C. Leung and F. K. Lam, "Image segmentation using maximum entropy method," in *Proc. IEEE, Int. Symp. Speech, Image Process. Neural Netw.*, Apr. 1994, pp. 29–32.
[47] D. Feng, S. Wenkang, C. Liangzhou, D. Yong, and Z. Zhenfu, "Infrared image segmentation with 2-D maximum entropy method based on particle swarm optimization (PSO)," *Pattern Recognit. Lett.*, vol. 26, no. 5, pp. 597–603, Apr. 2005.
[48] L. M. Pickett, J. Manin, R. Payri, M. Bardi, and J. Gimeno, "Transient rate of injection effects on spray development," SAE Tech. Paper 0001, 2013.

[49] W. E. Eagle, L.-M. Malbec, and M. P. Musculus, "Measurements of liquid length, vapor penetration, ignition delay, and flame lift-off length for the engine combustion network 'spray B' in a 2.34 L heavy-duty optical diesel engine," *SAE Int. J. Engines*, vol. 9, no. 2, pp. 910–931, Jun. 2016.
[50] A. Zhang, A. Montanaro, L. Allocca, J. Naber, and S.-Y. Lee, "Measurement of diesel spray formation and combustion upon different nozzle geometry using hybrid imaging technique," *SAE Int. J. Engines*, vol. 7, no. 2, pp. 1034–1043, Jul. 2014.
[51] J. Wang, E. M. Mirynowski, J. A. Bittle, and B. T. Fisher, "Experimental measurements of n-heptane liquid penetration distance and spray cone angle for steady conditions relevant to early direct-injection low-temperature combustion in diesel engines," *Int. J. Engine Res.*, vol. 17, no. 4, pp. 371–390, Apr. 2016.
[52] Y. Park, J. Hwang, C. Bae, K. Kim, J. Lee, and S. Pyo, "Effects of diesel fuel temperature on fuel flow and spray characteristics," *Fuel*, vol. 162, pp. 1–7, Dec. 2015.
[53] J. Tian, M. Zhao, W. Long, K. Nishida, T. Fujikawa, and W. Zhang, "Experimental study on spray characteristics under ultra-high injection pressure for DISI engines," *Fuel*, vol. 186, pp. 365–374, Dec. 2016.
[54] P. J. Tennison, T. L. Georjon, P. V. Farrell, and R. D. Reitz, "An experimental and numerical study of sprays from a common rail injection system for use in an HSDI diesel engine," SAE Tech. Paper 724, 1998.
[55] C. Grimaldi and L. Postrioti, "Experimental comparison between conventional and bio-derived fuels sprays from a common rail injection system," *SAE Int.*, vol. 109, no. 3, pp. 1501–1513, 2000.
[56] L. Araneo, A. Coghe, G. Brunello, and G. E. Cossali, "Experimental investigation of gas density effects on diesel spray penetration and entrainment," SAE Tech. Paper 0525, 1999.
[57] V. Bermúdez, R. Payri, F. J. Salvador, and A. H. Plazas, "Study of the influence of nozzle seat type on injection rate and spray behaviour," *Inst. Mech. Eng., D, J. Automobile Eng.*, vol. 219, no. 5, pp. 677–689, May 2005.
[58] J. Benajes, F. J. Salvador, M. Carreres, and D. Jaramillo, "On the relation between the external structure and the internal characteristics in the near-nozzle field of diesel sprays," *Inst. Mech. Eng., D, J. Automobile Eng.*, vol. 231, no. 3, pp. 360–371, Apr. 2017.
[59] D. L. Hung *et al.*, "Gasoline fuel injector spray measurement and characterization—A new SAE J2715 recommended practice," *SAE Int. J. Fuels Lubricants*, vol. 1, no. 1, pp. 534–548, 2009.
[60] L. C. Ganippa, G. Bark, S. Andersson, and J. Chomiak, "Cavitation: A contributory factor in the transition from symmetric to asymmetric jets in cross-flow nozzles," *Experim. Fluids*, vol. 36, no. 4, pp. 627–634, Apr. 2004.
[61] H. Hiroyasu and H. Miao, "Measurement and calculation of diesel spray penetration," in *Proc. ICLASS Conf.*, 2003, pp. 1–8.
[62] R. Masuda, T. Fuyuto, M. Nagaoka, E. Von Berg, and R. Tatschl, "Validation of diesel fuel spray and mixture formation from nozzle internal flow calculation," SAE Tech. Paper 2098, May 2005.
[63] S. Moon, K. Nishida, Y. Matsumoto, and J. Lee, "Gas entrainment characteristics of diesel spray during end of injection transient," *Atomization Sprays*, vol. 19, no. 11, pp. 1013–1029, 2009.
[64] K. J. Wu, C. C. Su, R. L. Steinberge, D. A. Santavicca, and F. V. Bracco, "Measurements of the spray angle of atomizing jets," *J. Fluids Eng.*, vol. 105, no. 4, pp. 406–413, Dec. 1981.

IRENE RUIZ-RODRIGUEZ received the M.Eng. degree in aerospace engineering from Brunel University London, U.K., in 2016, where she is currently pursuing the Ph.D. degree. Her research interests include sprays and combustion fundamentals, and optical analysis and diagnostics of them. She is an Associate Member of the Institution of Mechanical Engineers and an Associate Fellow of the Higher Education Academy.

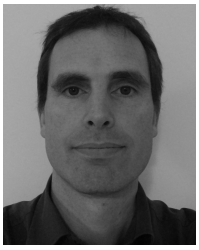

RADBOUD POS received the B.Sc. and M.Sc. degrees in physics from the University of Utrecht, The Netherlands, in 2012, and the Ph.D. degree in mechanical engineering from Brunel University London, where the subject of his study was the spatio-temporal evolution of diesel sprays from the used injectors. He is currently a Health Physicist with the Delft University of Technology, The Netherlands.

THANOS MEGARITIS is currently a Professor in mechanical and aerospace engineering with Brunel University London. His research interests include engine combustion and emissions, exhaust gas after treatment, fuel reforming, and alternative fuels. He is a Fellow of the Institution of Mechanical Engineers and a member of the Society of Automotive Engineers.

LIONEL CHRISTOPHER GANIPPA is currently a Professor in mechanical and aerospace engineering with Brunel University London. His research interests include diesel sprays, engine combustion and emission performance, alternative fuels, and soot diagnostics. He is a U.K. Chartered Engineer and a Fellow of the Institution of Mechanical Engineers, U.K., and the Higher Education Academy.